

Computation and analysis of light emission in two-bubble sonoluminescence

Jin-Fu Liang(梁金福), Xue-You Wu(吴学由), Yu An(安宇), Wei-Zhong Chen(陈伟中), Jun Wang(王军)

Citation: Chin. Phys. B . 2020, 29(9): 097801 . **doi:** 10.1088/1674-1056/ab969e
Journal homepage: http://cpb.iphy.ac.cn; http://iopscience.iop.org/cpb

What follows is a list of articles you may be interested in

Extinction mechanisms of hyperbolic h-BN nanodisk

Runkun Chen(陈闰堃), Jianing Chen(陈佳宁)

Chin. Phys. B . 2020, 29(5): 057802 . **doi:** 10.1088/1674-1056/ab8898

Spectral properties of Pr:CNGG crystals grown by micro-pulling-down method

Yan-Yan Xue(薛艳艳), Na Li(李纳), Dong-Hua Hu(胡冬华), Qing-Song Song(宋青松), Xiao-Dong Xu(徐晓东), Dong-Hai Wang(王东海), Qing-Guo Wang(王庆国), Dong-Zhen Li(李东振), Zhan-Shan Wang(王占山), Jun Xu(徐军)

Chin. Phys. B . 2019, 28(8): 087801 . **doi:** 10.1088/1674-1056/28/8/087801

Influence of annealing treatment on the luminescent properties of Ta:β-Ga_2O_3 single crystal

Xiaowei Yu(余小威), Huiayuan Cui(崔慧源), Maodong Zhu(朱茂东), Zhilin Xia(夏志林), Qinglin Sai(赛青林)

Chin. Phys. B . 2019, 28(7): 077801 . **doi:** 10.1088/1674-1056/28/7/077801

Spectra properties of Yb^{3+}, Er^{3+}: Sc_2SiO_5 crystal

Yanyan Xue(薛艳艳), Lihe Zheng(郑丽和), Dapeng Jiang(姜大朋), Qinglin Sai(赛青林), Liangbi Su(苏良碧), Jun Xu(徐军)

Chin. Phys. B . 2019, 28(3): 037802 . **doi:** 10.1088/1674-1056/28/3/037802

Crystal growth and spectral properties of Tb: Lu_2O_3

Jiaojiao Shi(施佼佼), Bin Liu(刘斌), Qingguo Wang(王庆国), Huili Tang(唐慧丽), Feng Wu(吴锋), Dongzhen Li(李东振), Hengyu Zhao(赵衡煜), Zhanshan Wang(王占山), Wen Deng(邓文), Xu Zian(徐子安), Xu Jiayue(徐家跃), Xiaodong Xu(徐晓东), Jun Xu(徐军)

Chin. Phys. B . 2018, 27(9): 097801 . **doi:** 10.1088/1674-1056/27/9/097801

Computation and analysis of light emission in two-bubble sonoluminescence*

Jin-Fu Liang(梁金福)[1,†], Xue-You Wu(吴学由)[1], Yu An(安宇)[2], Wei-Zhong Chen(陈伟中)[3], and Jun Wang(王军)[4]

[1] School of Physics and Electronic Science, Guizhou Normal University, Guiyang 550025, China
[2] Department of Physics, Tsinghua University, Beijing 100084, China
[3] Institution of Acoustics, Nanjing University, Nanjing 210093, China
[4] School of Chemistry and Materials Science, Guizhou Normal University, Guiyang 550025, China

(Received 11 April 2020; revised manuscript received 11 May 2020; accepted manuscript online 27 May 2020)

We perform a computational simulation of light emissions from two sonoluminescent bubbles in water. Our simulation includes the radii of two bubbles, radiation acoustic pressures, and light emission spectra by numerically solving the pulsing equations of a two-bubble system and the equations of gas dynamics. The simulation results demonstrate that the motion of each bubble in the two-bubble system is restrained because of the radiation acoustic pressures from the other pulsing bubble. The restrained oscillation of a bubble with a small ambient radius is stronger than that of a bubble with a large ambient radius under the same driving acoustic pressure. This effect increases when the distance between the two bubbles decreases. When compared to single-bubble sonoluminescence, the interaction between two bubbles leads to generation of different spectral characteristics.

Keywords: two-bubble sonoluminescence, radiation acoustic pressure, spectra

PACS: 78.60.Mq, 47.55.dd, 43.35.+d **DOI:** 10.1088/1674-1056/ab969e

1. Introduction

Sonoluminescence (SL) is a light emission phenomenon resulting from extreme temperatures and pressures achieved during the violent collapse of gas bubbles in liquids irradiated with high-intensity ultrasound waves.[1–4] SL can occur either from a single isolated cavitating bubble (i.e., single-bubble SL, SBSL)[5] or from a cloud of cavitation bubbles (i.e., multi-bubble SL, MBSL).[6] In experiment, each individual bubble tends to be dimmer during MBSL than during SBSL, although the input power for MBSL is much higher than that for SBSL. It is roughly understood that each of the bubbles shares the input energy during the MBSL so that the energy is distributed among the individual bubbles, and ultimately may be smaller than the energy input for SBSL.[7] However, the details of the dynamic process of energy distribution in a multi-bubble system are unclear.

An MBSL system is rather complex. In addition to being a many-body problem with the interaction between cavitation bubbles and the nonlinear motion of each individual bubble, the life of each individual cavitation bubble is uncertain. Moreover, a multi-bubble system includes various structures, such as filaments (streamers),[8] clusters (bubble grapes),[9] and other such patterns. Therefore, it is virtually impossible to directly simulate the cavitation process for a multi-bubble system.

For structures consisting of cavitation bubbles, a two-bubble system is an important unit in that it is not only simple but also includes the clues of interaction between two bubbles, which helps in detailedly understanding the MBSL phenomenon by investigating the two-bubble system.

Many researchers have investigated the dynamics of a two-bubble system, both theoretically and experimentally. In 1906, Bjerknes first discovered the acoustic radiation force acting on bubbles.[10] This force, called the Bjerknes force today, results from a spatial pressure gradient, and is categorized into primary and secondary Bjerknes forces. The former is caused by the primary external wave, and the latter is caused by the vibrating bubbles. The secondary Bjerknes force generally denotes the mutual force among bubbles. In 1975, Crum developed a simple model for the secondary Bjerknes force between two bubbles, assuming that the radii of the bubbles linearly vibrated with a small amplitude.[11] In 1990, Oguz *et al.* conducted numerical simulations of a nonlinear model of two vibrating and translating bubbles and demonstrated that increasing the acoustic force can even reverse the direction of the force.[12] In 1997, Mettin *et al.* numerically investigated the mutual interaction between bubbles with smaller oscillations in a strong acoustic field.[13] In 1999, Doinikov derived a formula for the secondary Bjerknes force between two bubbles in a viscous compressible liquid.[14] Moreover, he discussed the viscous effect on mutual force and pointed out that the effects can cause smaller bubbles to be driven well below

*Project supported by the National Natural Science Foundation of China (Grant Nos. 11864007 and 11564006) and the Science and Technology Planning Project of Guizhou Province of China (Grant No. [2018]5769).

†Corresponding author. E-mail: liang.shi2007@163.com

© 2020 Chinese Physical Society and IOP Publishing Ltd

resonance.[15] Barbat *et al.*[16] experimentally observed that two bubbles can undergo a stable and periodic translational motion. More recently, Rasoul *et al.*[17] numerically studied the influence of various concentrations of sulfuric acid on the interaction between two oscillating sonoluminescent bubbles. Based on Lagrangian mechanics, Eruihara *et al.*[18] theoretically investigated the dynamics of two interacting axisymmetric spherical bubbles with small deformed shapes. The authors of Refs. [19,20] also used the perturbation theory and the potential flow formula to numerically investigate the dynamics of two interacting bubbles in a non-spherical ultrasound field.

The intense pulsing of two bubbles may lead to an extremely high temperature and pressure, which may lead to the dissociation and ionization of gas atoms and molecules inside a bubble, ultimately resulting in light emission (we define this as two-bubble sonoluminescence (TBSL) in this paper), which may be similar to SBSL. However, very few reports on the of TBSL can be seen in literature. The aim of this paper is to discuss the effect of the mutual force between two bubbles on light emission by numerically calculating the dynamical model of coupled vibrations of two bubbles and a light emission model of SBSL.

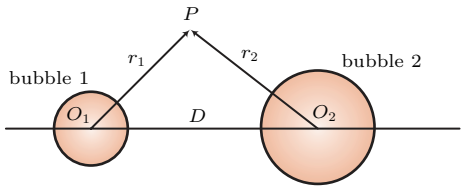


Fig. 1. Geometry of two interacting cavitation bubbles with different ambient radii.

2. Theoretical model

2.1. Equation of two-bubble dynamics

In the present study, we consider two spherical argon bubbles in perfectly incompressible water, as shown in Fig. 1. After ignoring the rotation of the liquid, the deformation of bubbles, and the spatial movement of the bubbles, the equations of the two-bubble system are described as follows:[19–21]

$$R_1\ddot{R}_1+\frac{3}{2}\dot{R}_1^2+\frac{1}{D}(R_2^2\ddot{R}_2+2R_2\dot{R}_2^2)=\frac{1}{\rho_1}[p(r_1)-p(\infty)], \quad (1)$$

$$R_2\ddot{R}_2+\frac{3}{2}\dot{R}_2^2+\frac{1}{D}(R_1^2\ddot{R}_1+2R_1\dot{R}_1^2)=\frac{1}{\rho_1}[p(r_2)-p(\infty)], \quad (2)$$

$$p(r_1)\big|_{r_1=R_1}=p_{g1}-p_0-\frac{2\sigma}{R_1}-\frac{4\eta}{R_1}\dot{R}_1+\frac{R_1}{c}\frac{\mathrm{d}}{\mathrm{d}t}[p_{g1}-p_d(t)]-p_d(t), \quad (3)$$

$$p(r_2)\big|_{r_2=R_2}=p_{g2}-p_0-\frac{2\sigma}{R_2}-\frac{4\eta}{R_2}\dot{R}_2+\frac{R_2}{c}\frac{\mathrm{d}}{\mathrm{d}t}[p_{g2}-p_d(t)]-p_d(t), \quad (4)$$

Considering the adiabatic approximation for two bubbles, we can obtain

$$p_{g1}=\left(p_0+\frac{2\sigma}{R_{10}}\right)\left(\frac{R_{10}^3-h_1^3}{R_1^3-h_1^3}\right)^{\gamma}, \quad (5)$$

$$p_{g2}=\left(p_0+\frac{2\sigma}{R_{20}}\right)\left(\frac{R_{20}^3-h_2^3}{R_2^3-h_2^3}\right)^{\gamma}, \quad (6)$$

where ρ_1 is the density of the liquid, $p(\infty)$ denotes the infinite in liquid, p_0 is the static pressure in the liquid (we set $p(\infty)=p_0$ in this paper), η is the viscosity, σ is the surface tension, c is the speed of sound in a liquid, γ is the ratio of specific heats, and h_1 and h_2 are the collective hard cores of van der Waal's volume, with $h_1=R_{10}/8.5$ for bubble 1 and $h_2=R_{20}/8.5$ for bubble 2. R_{10} and R_{20} are the ambient radii for bubbles 1 and 2, respectively.

During the pulsing of bubble 1, the driving force includes not only the external driving acoustic pressure $p_d(t)=-p_a\sin(\omega t)$ and the initial ambient pressure $p_0=p(\infty)$, but also the radiation acoustic pressure p_{int1} from bubble 2. Similarly, bubble 2 is also affected by the radiation acoustic pressure p_{int2} from bubble 1. Assuming each of two bubbles as the noise source of the monopole, according to the equation of acoustic pressure[21,22]

$$\nabla^2 p-c^2\ddot{p}=-\dot{q}, \quad (7)$$

the radiation acoustic pressures from bubbles 1 and 2 read

$$p_{rad1}=\frac{\rho_1}{r_1}[2R_1(\tau_1)\dot{R}_1^2(\tau_1)+R_1^2(\tau_1)\ddot{R}_1(\tau_1)], \quad (8)$$

$$p_{rad2}=\frac{\rho_1}{r_2}[2R_2(\tau_2)\dot{R}_2^2(\tau_2)+R_2^2(\tau_2)\ddot{R}_2(\tau_2)]. \quad (9)$$

Therefore,

$$p_{int1}=\frac{\rho_1}{D}[2R_2(\tau)\dot{R}_2^2(\tau)+R_2^2(\tau)\ddot{R}_2(\tau)], \quad (10)$$

$$p_{int2}=\frac{\rho_1}{D}[2R_1(\tau)\dot{R}_1^2(\tau)+R_1^2(\tau)\ddot{R}_1(\tau)], \quad (11)$$

where $\tau=t-D/c$.

2.2. Formula of light emission in TBSL

We employed the theoretical model described in Refs. [23–27] for SBSL to simulate the light emission spectra in TBSL. In this model, the boundary at the moving bubble wall is still expressed by Eqs. (1) and (2). However, the adiabatic approximation is no longer valid, and the pressure for driving one bubble is not only $p_d(t)$, but also the radiation pressure from the other bubble.

In this paper, we consider only two types of gas components: argon gas and water vapor inside the bubble. The dynamics of the gas component inside each bubble may be described by the following partial differential equation (PDE) of

fluid mechanics:[23]

$$\begin{cases} \dfrac{\partial \rho_1}{\partial t}+\dfrac{1}{r^2}\dfrac{\partial}{\partial r}[r^2(\rho_1 \upsilon_1+J_1)]=0, \\ \dfrac{\partial \rho}{\partial t}+\dfrac{1}{r^2}\dfrac{\partial}{\partial r}(r^2\rho\upsilon)=0, \\ \dfrac{\partial(\rho\upsilon)}{\partial t}+\dfrac{1}{r^2}\dfrac{\partial}{\partial r}(r^2\rho\upsilon^2)+\dfrac{\partial p}{\partial r}=\dfrac{1}{r^2}\dfrac{\partial}{\partial r}(r^2\tau_{\rm rr})+\dfrac{\tau_{\rm rr}}{r}, \\ \dfrac{\partial E}{\partial t}+\dfrac{1}{r^2}\dfrac{\partial}{\partial r}\{r^2[(E+p)\upsilon+q]\}=\dfrac{1}{r^2}\dfrac{\partial}{\partial r}(r^2\upsilon\tau_{\rm rr}), \end{cases} \tag{12}$$

where t is the time, r is the radial coordinate, ρ_i is the density of the i-th gas, $\rho=\rho_1+\rho_2$ is the density of the gas mixture, υ_1 is the radial component of the i-th gas velocity, υ is the average velocity, $\rho\upsilon=\rho_1\upsilon_1+\rho_2\upsilon_2$, p is the gas pressure, q is the heat flux, J_1 is the diffusion mass flux of species 1 (the vapor) with respect to the average velocity, $J_1=\rho_1(\upsilon_1-\upsilon)$, $\tau_{\rm rr}=(4\mu/3)\times(\partial\upsilon/\partial r-\upsilon/r)$, $E=E_1+E_2$, the total energy density, $E_i=\rho_i\upsilon_i^2/2+\rho_i e_i$, and e_i is the internal energy of the i-th gas.

Once the temperature and pressure are sufficiently high during bubble collapse, the products after chemical dissociation such as OH radicals, hydrogen atoms, and oxygen atoms can be generated as well as in those processes of ionized positive and negative ions and electrons.[23]

We consider electron-ion bremsstrahlung, electron-atom bremsstrahlung, recombination radiation, and radiative attachment of electrons to some products of chemical reactions, such as O and H atoms and O_2 or OH molecules. Moreover, the line emission from the transition $A^2\Sigma^+\rightarrow X^2\Pi_i$ of OH radicals is also considered.[28] The formula of radiation power from each of the two bubbles is taken from[25]

$$P_\lambda(t)=8\pi^2\int_0^R\int_{-1}^1 k_\lambda(r)P_\lambda^{\rm PI}(r)\times\exp\left(-\int_{r_x}^{\sqrt{R^2-r^2(1-x^2)}}k_\lambda\,{\rm d}s\right)r^2\,{\rm d}r\,{\rm d}x, \tag{13}$$

which describes the total power emitted from each bubble of the two-bubble system for each acoustic cycle at wavelength λ. In this equation, r is the radial distance from the center of the bubble. $P_\lambda^{\rm PI}$ is the Plank radiation intensity, and k_λ the absorption coefficient.

The total radiation power is the integral over the relevant wavelengths λ.

$$P(t)=\int_{200\ {\rm nm}}^{900\ {\rm nm}}P(\lambda,t)\,{\rm d}\lambda. \tag{14}$$

The cumulative radiation energy emitted from each of the TBSL bubbles from time 0 to t within each acoustic period is

$$E_\lambda(t)=\int_0^t P(\lambda,t')\,{\rm d}t',\quad 0\le t\le\frac{2\pi}{\omega}. \tag{15}$$

3. Numerically calculated results

3.1. Motion and radiation acoustic pressures of two bubbles

The effects of the interaction between two bubbles are embodied in Eqs. (1) and (2). As a numerical trial, the present study arbitrarily sets $D=0.3$, 0.5, 1.0, and 2.0 mm, and the ambient radii of the two bubbles $R_{10}=4.5$ μm and $R_{20}=6.0$ μm, respectively. Based on the numerical calculation, we studied how the distance between bubbles affects their motion, and the characteristics of TBSL. All calculations assumed argon (Ar) bubbles in water at 20 °C, driven by acoustic waves with a frequency of 25 kHz.

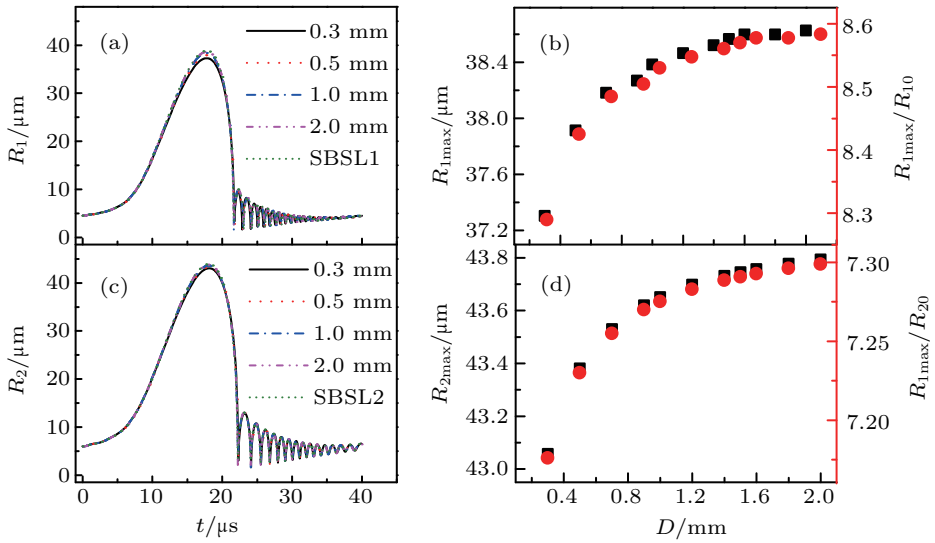


Fig. 2. (a) and (c) Radii of two argon bubbles as a function of time. The amplitude of the driving acoustic pressure is $p_{\rm a}=1.30$ atm, and the cases of 0.3, 0.5, 1.0, and 2.0 mm denote the distance between two bubbles, D. The cases of SBSL denote single isolated bubbles without any effect from the other bubble. (b) and (d) Maximum radii of the two bubbles, and the ratios of the maximum and ambient radii as a function of distance D.

Before calculating the light emission of a TBSL, we studied how the interaction between two bubbles affects their motions, and the radiation acoustic pressure of the two bubbles. Assuming that the pressure inside each bubble is an adiabatic approximation, we numerically solved Eqs. (1)–(6) and obtained the evolutions of radii of two bubbles with time, as shown in Figs. 2(a) and 2(c). Further, we found that the maximum radii ($R_{i\max}$, $i = 1$ or 2) of each bubble decrease as D decreases, and the ratios $R_{i\max}/R_{i0}$ of each bubble show a similar trend, as shown in Figs. 2(b) and 2(d). In general, the higher the value of $R_{i\max}/R_{i0}$, the stronger the intensity of light emission from a bubble.

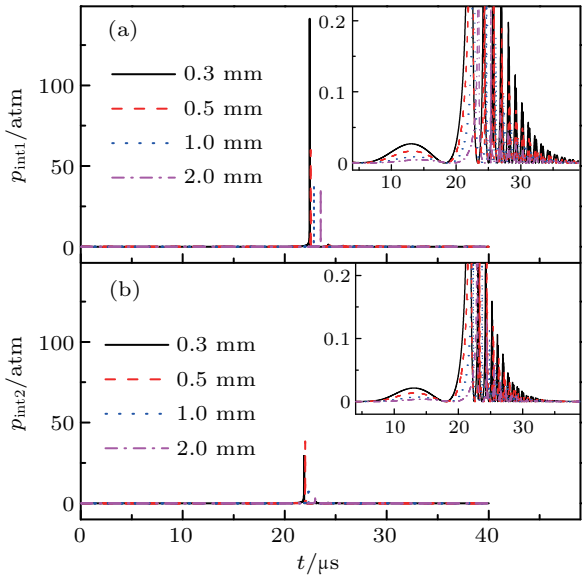


Fig. 3. Acoustic radiation pressures from other bubbles as a function of time: (a) bubble 1 with initial radius of 4.5 μm, (b) bubble 2 with initial radius of 6.0 μm. Here $p_{\rm a} = 1.30$ atm, and the cases of 0.3, 0.5, 1.0 and 2.0 mm denote different values of D, respectively.

Comparing Figs. 2(a) and 2(c) with Figs. 3(a) and 3(b), respectively, we can see that the acoustic radiation pressure from each bubble in a two-bubble system is positive when the bubble expands, and negative when it collapses. Consequently, the pressure prevents bubble expansion as it expands and prevents bubble compression as it is compressed. This effect is stronger when the value of D decreases (see Fig. 3).

In addition, the motion of each bubble in the two-bubble construction tends to restrain the motion of the other bubble. The oscillation of bubble 1 with a small ambient radius is more strongly restrained than that of bubble 2 with a large ambient radius under the same driving acoustic pressure. The interaction between two bubbles may generate different results for bubbles with different ambient radii, although the time scale of sharp peaks in the radiation pressure curve appears to be too short to have any visible effects on the bubble motion.

3.2. Spectral characteristics of TBSL

To understand the light emission characteristic of a TBSL, we employed the model developed in Refs. [23–26] for the case in which the bubble equation of motion is replaced by Eqs. (1) and (2). In this case, the adiabatic approximation is no longer valid. The gas dynamics inside the bubbles are determined by Eq. (12). Since the interactions between bubbles restrain motion of each bubble, the spectra from each bubble may appear to have different characteristics.

When comparing TBSL with $D = 0.3$, 0.5, 0.8, 1.0, 1.5, and 2.0 mm to SBSL ($D = \infty$), it is clear that each bubble in TBSL is dimmer than that of SBSL under the same driving acoustic pressure (see Figs. 4(a) and 5(a)). However, when $D \geq 1.5$ mm, the intensity of the spectra from TBSL is nearly equal to that from SBSL, which shows that TBSL is similar to two SBSLs when $D \geq 1.5$ mm.

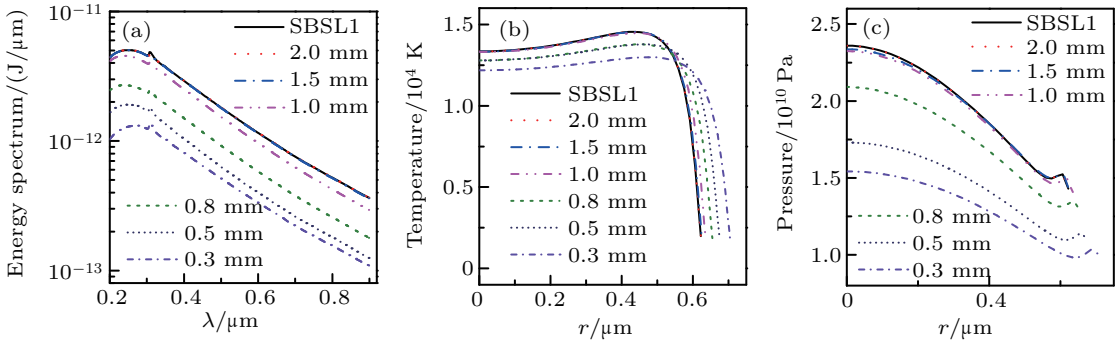


Fig. 4. Bubble 1 with ambient radius of 4.5 μm at different distances D from the other bubble 2 with ambient radius 6.0 μm. (a) Energy spectra, (b) temperature when the bubble reaches its minimum size, and (c) corresponding pressure. Here $p_{\rm a} = 1.30$ atm and the cases of 0.3, 0.5, 0.8, 1.0, 1.5 and 2.0 mm denote different values of D, respectively. SBSL1 denotes the cases of single isolated bubbles with ambient radius of 4.5 μm without any effect from other bubbles.

To further understand the process behind the appearance of the spectra, we simulated the light emission pulses and the radiation energy spectra from bubbles 1 and 2. The distributions of the temperatures and pressures inside bubbles 1 and 2 were also simulated.

Figure 6(a) illustrates the total radiation power per flash of bubble 1, and we selected eight moments (points A–H) on the curve to evaluate the radiation energy spectrum (Fig. 6(b))

and the corresponding temperature and pressure (Figs. 6(c) and 6(d)) for moments. The total intensity increases over each moment because of the accumulation of radiation energy over time. As the radiation power increases from A to H, the intensity of the continuum background increases, and the OH spectral peaks in the 0.30–0.40 μm region and gradually disappear. The central wavelength for OH emission ($A^2\Sigma^+ \rightarrow X^2\Pi_i$) are approximately 0.31 μm (0–0) and 0.34 μm (0–1), respectively (Fig. 6(b)). At the moment marked by H, the bubble ceases to luminesce, and the corresponding energy spectrum equals the accumulated spectrum during a single flash over one acoustic period.

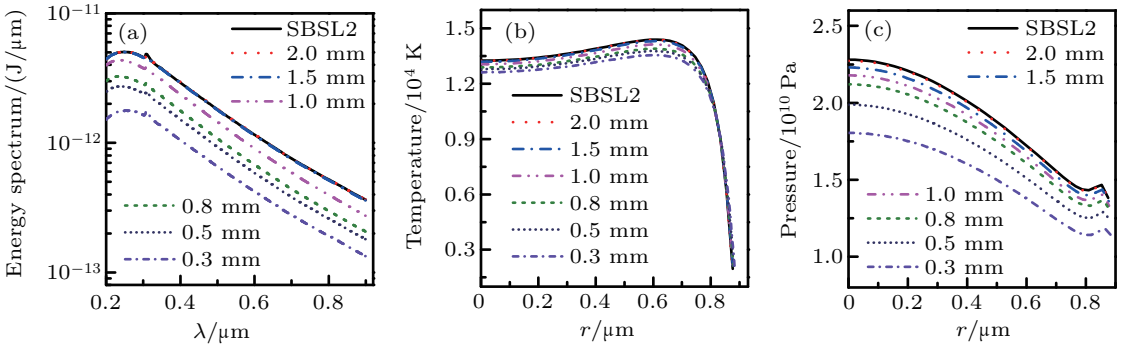


Fig. 5. Bubble 2 with ambient radius of 6.0 μm at different distances D from the other bubble 1 with ambient radius 4.5 μm. (a) Energy spectra, (b) Temperature when the bubble reaches its minimum size, and (c) corresponding pressure. $p_a = 1.30$ atm and the cases of 0.3, 0.5, 0.8, 1.0, 1.5 and 2.0 mm denote different values of D, respectively. SBSL2 denotes the cases of single isolate bubbles with initial radius of 6.0 μm without any effect from the other bubble.

The intensity of light emission is closer to the temperature inside the bubble. Figure 6(b) shows that under the same driving acoustic pressure amplitude $p_a = 1.30$ atm, the distribution of temperatures inside bubble 1 is at its minimum for different values of D. The maximum temperature increases with an increase in D between the two bubbles. With increasing temperature, the line emission peaks of OH disappear in the background continuum, which is similar to that of SBSL.[23,24] The results show that there is no essential difference between TBSL and SBSL, as both are related to hot and dense gas light emission.

To illustrate the ionization in each bubble in two-bubble system, we used the method reported in Refs. [29,30] to calculate the degree of ionization (α). Figures 8(a) and 8(b) illustrate the temporal profiles of the degree of ionization in bubbles 1 and 2, respectively. In Figs. 8(a) and 8(b), α decreases when (D) decreases, showing that the interaction between two bubbles decreases the α in each bubble in the two-bubble system. The reason for this may be that the temperatures in the two bubbles decrease when D decreases.

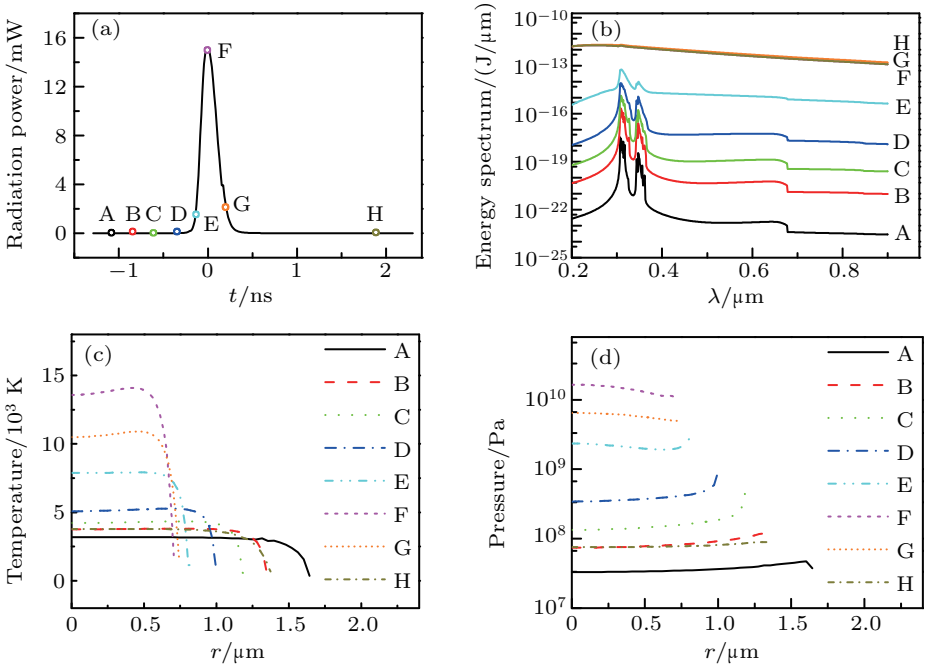


Fig. 6. Simulation results for bubble 1 with an ambient radius of 4.5 μm at distance $D = 0.3$ mm from bubble 2 with an ambient radius of 6.0 μm. The amplitude of the driving pressure $p_a = 1.30$ atm. (a) Radiation power of bubble 1 versus time, (b) energy spectra, (c) temperature, and (d) pressure.

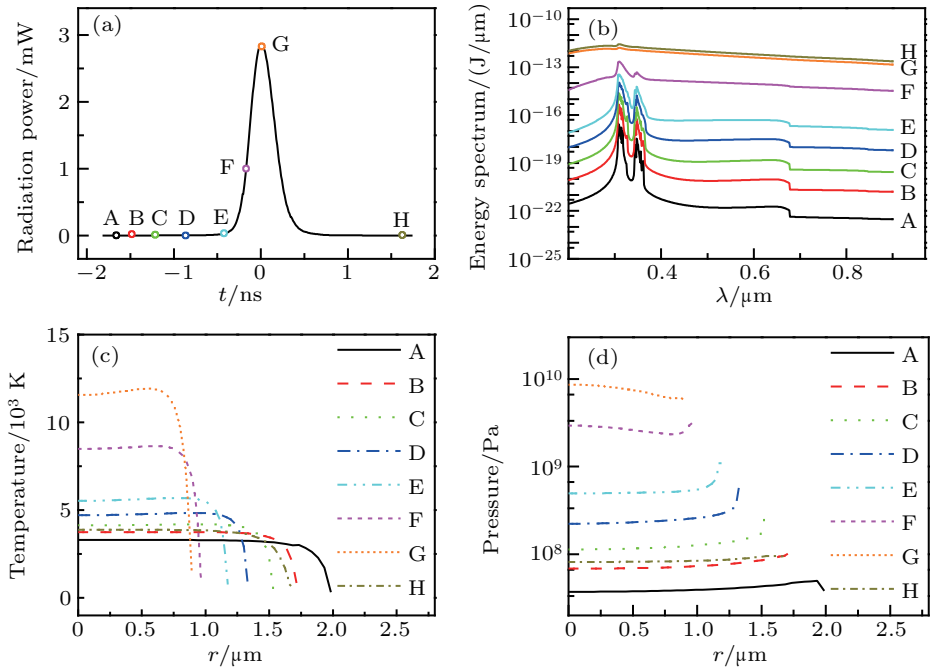


Fig. 7. Simulation results for bubble 2 with an ambient radius of 6.0 μm at distance $D = 0.3$ mm from bubble 1 with an ambient radius of 4.5 μm. The amplitude of the driving pressure $p_a = 1.30$ atm. (a) Radiation power of bubble 2 versus time, (b) energy spectra, (c) temperature, and (d) pressure.

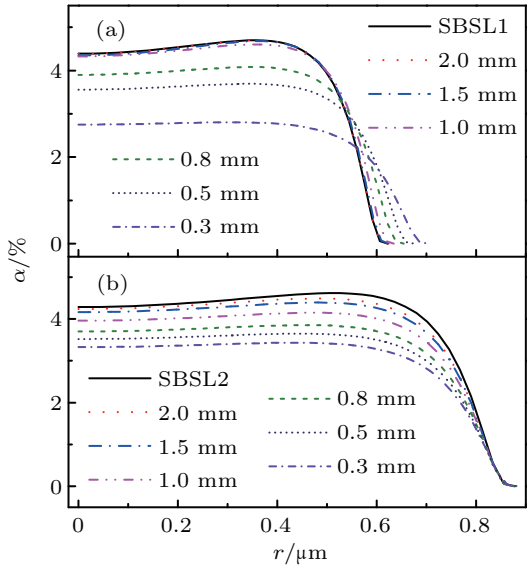


Fig. 8. Simulation results of the degree of ionization (α) inside two sonoluminescing bubbles at different D: (a) bubble 1 with an ambient radius of 4.5 μm, (b) bubble 2 with an ambient radius 6.0 μm.

4. Conclusion

In summary, we have numerically computed the motions of two Ar bubbles in water by an intense ultrasound wave, the radiation acoustic pressure, and the light emission spectra from two bubbles. The results demonstrate that the interaction between two bubbles originating from the radiation acoustic pressure suppresses bubble expansion and the extent of the bubble violent collapse. When the distance between two bubbles remains constant and the bubbles are under the same driving acoustic pressure, the smaller bubble 1 is suppressed more strongly than the larger bubble 2. The characteristics of the two-bubble luminescent spectrum depend only on the extreme conditions inside the bubbles, which is similar to SBSL. The extreme conditions inside each TBSL bubble depend on the distance between two bubbles, the ambient radius, and the intensity of the driving acoustic pressure. However, TBSL is difficult to obtain experimentally. For TBSL, many parameters such as the distance between two bubbles, sound pressure, gas concentration of liquid, environmental temperature, etc., are more sensitive than those for SBSL because of the interaction between two bubbles. Therefore, TBSL requires further experimental investigation.

References

[1] Putterman S J and Weninger K R 2000 *Annu. Rev. Fluid Mech.* **32** 445
[2] Suslick K S, Eddingsaas N C, Flannigan D J, Hopkins S D and Xu H 2018 *Acc. Chem. Res.* **51** 2169
[3] Brenner M P, Hilgenfeldt S and Lohse D 2002 *Rev. Mod. Phys.* **74** 425
[4] Suslick K S and Flannigan D J 2008 *Annu. Rev. Phys. Chem.* **59** 659
[5] Gaitan D F, Crum L A, Church C C and Roy R A 1992 *J. Acoust. Soc. Am.* **91** 3166
[6] Frenzel H and Schultes H 1934 *Z. Phys. Chem. B* **27** 421
[7] An Y 2011 *Phys. Rev. E* **83** 066313
[8] Neppiras E A 1980 *Phys. Rep.* **61** 159
[9] Flannigan D J and Suslick K S 2012 *J. Phys. Chem. Lett.* **3** 2401
[10] Bjerknes V 1906 *Fields of Force* (New York: Columbia University Press)
[11] Crum L 1975 *J. Acoust. Soc. Am.* **57** 1363
[12] Oguz H N and Prosperetti A 1990 *J. Fluids Mech.* **218** 143
[13] Mettin R, Akhatov I, Parlitz U, Ohl C D and Lauterborn W 1997 *Phys. Rev. E* **56** 2924
[14] Doinikov A A 1999 *J. Acoust. Soc. Am.* **106** 3305
[15] Doinikov A A 2002 *J. Acoust. Soc. Am.* **111** 1602
[16] Barbat T, Ashgriz N and Liu C S 1999 *J. Fluid Mech.* **389** 137
[17] Rasoul S B, Nastaran R, Homa E and Mona M 2010 *Phys. Rev. E* **82** 016316

[18] Eruihara K, Hay T A, Ilinskii Y, Zabolotskaya E and Hamilton M 2011 *J. Acoust. Soc. Am.* **130** 3357
[19] Liang J, Chen W Z, Shao W H and Qi S B 2012 *Chin. Phys. Lett.* **29** 074701
[20] Liang J, Wang X, Yang J and Gong L 2017 *Ultrasonics* **75** 58
[21] Pu Z, Zhang W, Shi K R, Zhang J H and Wu Y L 2005 *J. Tsinghua University* **45** 1450 (in Chinese)
[22] Ross D 1976 *Mechanics of Under Water Noise* (New York: Pergamon Press)
[23] An Y 2006 *Phys. Rev. E* **74** 026304
[24] An Y and Li C 2008 *Phys. Rev. E* **78** 046313
[25] An Y and Li C 2009 *Phys. Rev. E* **80** 046320
[26] Liang J and An Y 2017 *Phys. Rev. E* **96** 063118
[27] Liang J, An Y and Chen W 2019 *Ultrason. Sonochem.* **58** 104688
[28] Pflieger R, Brau H P and Nikitenko S 2010 *Chem. Eur. J.* **16** 11801
[29] Yasui K 2001 *Phys. Rev. E* **64** 016310
[30] Zhang W J and An Y 2015 *Chin. Phys. B* **24** 047802